Chemical Engineering Journal 547 (2026) 180743

Contents lists available at ScienceDirect

Chemical Engineering Journal

journal homepage: www.elsevier.com/locate/cej

Nitrogen valorization via autotrophic nitrous oxide production in a partial nitritation sequencing batch biofilm reactor

Lluc Olmo, Julio Pérez, Julián Carrera *

GENOCOV research group, Department of Chemical, Biological and Environmental Engineering, Universitat Autònoma de Barcelona, Spain

ARTICLE INFO

Keywords:
Waste resource recovery facility
Waste valorization
Nitrous oxide emissions
CANDO

ABSTRACT

Autotrophic nitrous oxide (N_2O) production was intentionally enhanced in a partial nitritation sequencing batch biofilm reactor (PN-SBBR) treating high-strength ammonium wastewater (1000 mg $N–NH_4^+$ L^{-1}). Reactor performance was evaluated under three pH conditions (6.8, 7.3, and 7.8), which strongly influenced N_2O production rates (97, 230, and 132 mg $N–N_2O$ L^{-1} d^{-1}, respectively) while maintaining similar ammonia oxidation rates (0.79–0.86 g $N–NH_4^+$ L^{-1} d^{-1}). Combined analysis of N_2O production, emission factor, and hydroxylamine accumulation identified pH 7.3 as the most favorable among the tested range for promoting N_2O formation under specific redox conditions. Operation with real reject water (from dewatering of digested sludge) further validated process robustness, increasing N_2O production by 38% and achieving a maximum conversion of 0.36 g $N–N_2O$ g^{-1} $N–NH_4^+$ oxidized. Mass and energy balance analysis demonstrated that integrating the PN-SBBR as a dedicated autotrophic N_2O production stage enables energy-efficient nitrogen valorization. Among the configurations evaluated, coupling PN-SBBR with Anammox provided the highest energy efficiency. Furthermore, incorporation of the autotrophic stage into Coupled Aerobic-anoxic Nitrous Decomposition Operation (CANDO)-based systems substantially improves their overall energy balance. These results demonstrate a viable route for energy recovery from ammonium-rich waste streams through controlled autotrophic N_2O production.

1. Introduction

The concept of the water resource recovery facility (WRRF) reframes wastewater treatment plants (WWTPs) as platforms for converting organic matter and nutrients into valuable products such as energy, fertilizers, biopolymers and chemical precursors [1,2]. Among existing technologies, anaerobic digestion is now widely implemented to recover chemical energy from organic matter, which represents the major fraction of theoretical energy potential of wastewater considering its composition (~3.9 kWh kg^{-1} Chemical Oxygen Demand, COD) [3].

The energy recovery from organic matter is well stablished, while nitrogenous compounds remain largely untapped as energy source. In conventional urban WWTP, nitrogen is removed through nitrification-denitrification (N/DN), an energy-intensive process (~7.5 kWh kg^{-1} Total Nitrogen, TN) requiring substantial aeration for ammonia and nitrite oxidation plus organic carbon for nitrate reduction [4,5]. To reduce these demands, shortcut nitrogen removal—partial nitritation (PN) mediated by ammonia-oxidizing bacteria (AOB)—has been proposed. Coupling PN with autotrophic Anammox process (PN/A) enhances energy efficiency by reducing the aeration energy demand and by eliminating the need for organic matter that can be redirected to the anaerobic digestion. However, shortcut pathways tend to increase nitrous oxide (N_2O) emissions during PN, mainly due to nitrite accumulation, carbon content or biofilm growth [6,7]. Despite the difficulties in reducing N_2O emissions, a large fraction of the nitrogen content in wastewater is eliminated as inert N_2 gas thus the PN/A process is basically considered as nutrient removal rather than nitrogen valorization.

Nitrous oxide itself is a potent oxidant and has long been used as fuel additive among other industrial and medical applications [8]. Due to its high combustion potential, the oxidation of methane with N_2O produces ca. 37% more energy than oxidation with O_2 [8]. This has driven increasing interest in nitrogen valorization through controlled N_2O production, with the Coupled Aerobic-anoxic Nitrous Decomposition Operation (CANDO) process emerging as the leading approach [9–11]. CANDO was designed to transform the ammonia nitrogen of the reject water from the dewatering of digested sludge into nitrous oxide. CANDO is a two-stage process: (i) firstly, in a PN reactor, the ammonia nitrogen

* Corresponding author.
E-mail address: julian.carrera@uab.cat (J. Carrera).

https://doi.org/10.1016/j.cej.2026.180743
Received 4 June 2026; Received in revised form 30 July 2026; Accepted 13 August 2026
Available online 14 August 2026
1385-8947/© 2026 The Authors. Published by Elsevier B.V. This is an open access article under the CC BY-NC-ND license (http://creativecommons.org/licenses/by-nc-nd/4.0/).

is completely oxidized to nitrite, (ii) secondly, in a heterotrophic denitritation reactor, the nitrite is reduced to N_2O by adding an external source of organic matter. However, diverting organic matter to N_2O production competes directly with anaerobic digestion, reducing the net energy yield [12].

To overcome this limitation, autotrophic N_2O production—especially via AOB in PN reactors—offers a promising alternative because it eliminates the consumption of organic matter. Exploiting AOB physiology to drive N_2O production during PN could shift nitrogen management from a removal paradigm towards true resource recovery.

The present study investigates how to maximize the autotrophic N_2O production in a partial nitritation sequencing batch biofilm reactor (PN-SBBR). A stable and significant autotrophic N_2O production would open a new way for the valorization of the nitrogen content of reject water from dewatering of digested sludge.

2. Materials and methods

2.1. Reactor description, operation and biomass characterization

An SBBR with 20 L capacity, an exchange volume ratio of 50% and mechanical stirring was fed during 280 days with synthetic wastewater. The composition of this wastewater was adapted from [13]: 5.6 g L^{-1} of NH_4HCO_3 (1 g N-NH_4^+ L^{-1}), 0.24 g L^{-1} of each K_2HPO_4 and KH_2PO_4 and 1.25 mL L^{-1} of trace element solution. The composition of this solution was adapted from [14] (19.11 g EDTA L^{-1}, 0.43 g $ZnSO_4{\cdot}7H_2O$ L^{-1}, 0.24 g $CoCl_2{\cdot}6H_2O$ L^{-1}, 1.0 g $MnCl_2{\cdot}4H_2O$ L^{-1}, 0.25 g $CuSO_4{\cdot}5H_2O$ L^{-1}, 0.22 g $(NH_4)_6Mo_7O_{24}{\cdot}4H_2O$ L^{-1}, 0.20 g $NiCl_2{\cdot}6H_2O$ L^{-1}, 0.09 g $NaHSeO_3$ L^{-1}, 0.014 g H_3BO_3 $L^{-1}$and 0.054 g $Na_2WO_4{\cdot}2H_2O$ L^{-1}). Subsequently, in a 30-days-period of operation, the SBBR was fed with reject water from an urban WWTP near Barcelona (Spain) with total COD, soluble COD and ammonium concentrations of 506 ± 12 mg COD L^{-1}, 382 ± 3 mg COD L^{-1} and 880 ± 10 mg N-NH_4^+ L^{-1}, respectively. During these 30 days, NH_4HCO_3 was added to the reject water to increase the ammonium concentration to the same level as the synthetic influent (1000 mg of N-NH_4^+ L^{-1}), thereby enabling direct comparison of reactor performance.

Prior to the experimental campaign, the reactor was initially inoculated with activated sludge from an urban wastewater treatment plant (Catalonia, Spain) and operated under PN conditions for more than one year, resulting in a *Nitrosomonas* abundance exceeding 55% [15]. A biofilm was then developed from this highly concentrated PN activated sludge (~3 g of Volatile Suspended Solids, VSS L^{-1}). During the start-up phase, this biofilm was formed by the spontaneous cell attachment to the submerged surfaces of the reactor. It was assumed that the biofilm reached quasi-steady-state growth after 60 days of immobilization, according to [16]. The biofilm reactor achieved a high biomass concentration (5 ± 1 g VSS L^{-1}), and the mature biofilm had a biofilm density of 17 ± 3 g VSS $L_{biofilm}^{-1}$ with 41 ± 5% of VSS/Total suspended solids ratio.

The pH, temperature and Dissolved Oxygen (DO) concentration were measured using online sensors. The bulk liquid pH was controlled and maintained, by dosing $KHCO_3$ 2 M solution, at setpoints of 7.8, 7.3 and 6.8 throughout the operational periods I, II and III, respectively. After completion of operational period III, the experiment was extended with an additional operational period (II-bis), during which pH was set back to a setpoint of 7.3 while maintaining the same synthetic influent composition of the previous periods. This step was performed to verify the stability and repeatability of the effect of pH on N_2O production. In the last operational period reported (period IV), the reactor was fed with real wastewater as described above, and the pH was maintained, by dosing $KHCO_3$ 2 M solution, at a pH setpoint of 7.3. Because the addition of ammonium bicarbonate altered the buffering capacity of the influent, the pH controller was re-tuned for period IV (i.e, a higher controller gain was set); nevertheless, the reactor pH remained stable within ±0.1 pH units of the target value throughout operation.

Throughout all the experimental periods, temperature was kept at 30 ± 1 °C by manually adjusting the serpentine heat exchanger temperature when needed. Compressed air was supplied through an air diffuser placed in the bottom of the reactor at a constant airflow of 420 L h^{-1}. The total cycle length was 24 h, corresponding to a hydraulic retention time (HRT) of 2 days and the cycle stages were distributed as depicted in Fig. 1. Firstly, aerated feeding started and 10 L of wastewater were added along 3.8 h and aerobic conditions were extended for 10 h. Then, three aeration and stirrer stops (interspersed settling) of 0.7 h each one were spread every 3.7 h across 8.2 h and finally, 4.8 h more of aerobic conditions completed the aeration stage. Subsequently, the final settling and decanting stage of 1 h took place and preceded the following cycle. This operational strategy was adopted for intentional enhancement of the N_2O production based on own previous experimental experience [15].

A moving average window was calculated ($n = 3$) throughout the operational period for nitrogen loading rate (NLR), ammonium oxidation rate (AOR), nitrite accumulation rate (NiAR), emission factor (EF) and nitrous oxide production rate (N2OR) to facilitate the identification of potential stable periods. The performance stability of each experimental period was evaluated using the coefficient of variation (CV), assuming the stability when the CV was lower than 10% [15,18].

Each determined stable phase was longer than five HRTs and after each pH setpoint change, an additional five HRTs period stablished a conservative transition stage for considering a stable phase. Period I was run from day 0 to 47 with a corresponding stable phase from day 21 to 47; period II from day 48 to 109 and stable phase from day 82 to 109; period III from day 110 to 173 and stable phase from day 151 to 173; period II-bis from day 174 to 278 and stable phase from day 209 to 244 and finally, period IV from day 280 to 311 and stable phase from days 296 and 311.

2.2. Chemical analyses, calculations and statistical analysis

Ammonium, nitrite and nitrate concentrations in influent and effluent were regularly measured off-line using both Hach Lange test kits (Hach Lange, Germany) and ion chromatography using ICS-2000 (DIONEX Corporation, USA) on samples previously filtered through 0.22 µm membranes. N_2O concentration in the gas phase was estimated based on the volumetric mass transfer coefficient ($K_L a_{N_2O}$) following a mathematically closed liquid-to-gas mass transfer modeling approach widely validated in wastewater literature [19,20], as detailed in the Supplementary data where the specific mass balance and rate calculations are outlined.

All calculations of AOR, NiAR, NLR, N2OR, as well as free nitrous acid (FNA) concentration, the emission factor based on oxidized nitrogen ($EF_{oxidized}$), and the emission factor based on nitrogen load (EF_{load}) are presented in detail in Supplementary data (Section 1). The N2OR was calculated as the sum of four different rates: During aerated stages of the cycle, the N2OR was divided into N2OR aerobic ($N2OR_{aer}$) and N2OR during aeration resumption causing N_2O peaks ($N2OR_{peak}$ and $N2OR_{extrapeak,}$ for the initial and the interspersed aeration resumptions, respectively). The $N2OR_{liq}$ accounted for the dissolved N_2O content in the liquid effluent.

Statistical significance of the experimental results was assessed using One-way ANOVA to evaluate the global effect of pH. Pairwise differences were identified via Welch's *t*-tests to account for heteroscedasticity, allowing for a reliable comparison of the mean performance of two separate operational periods while accounting for the differences in variance and potential background noise introduced by the long temporal gap. Statistical analysis details are provided in the Supplementary data (Section 2).

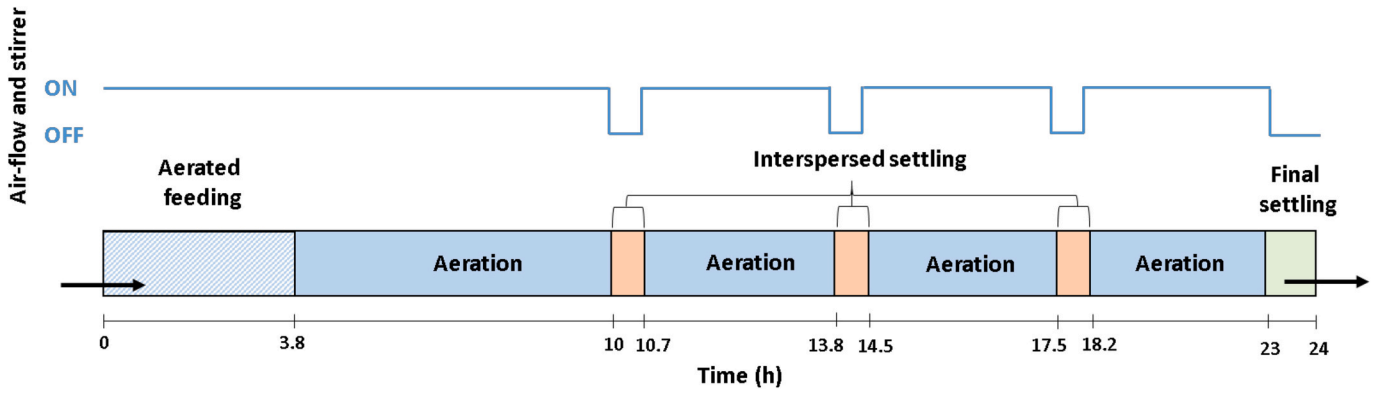


Fig. 1. Cycle stages during stable PN operation. Black arrows represent transition between consecutive cycles.

2.3. Microbiology characterization

Microbiological community composition was identified by using next-generation sequencing analysis. A biomass sample was extracted from the SBBR at the end of the stable phase of each period: I (day 47), II (day 105), III (day 173), II-bis (day 275) and IV (day 311). All samples were extracted by inserting a Pasteur pipette and scratching the biofilm to collect, approximately, 2 mL of sample in two separate Eppendorf tubes. DNA was extracted by using the Soil DNA Isolation Plus KitTM (Norgen Biotek Corp, Canada) following the manufacturing protocol. The quantity and quality of the extracted DNA was measured by using the NanoDrop 1000 Spectrophotometer (Thermo Fischer Scientific, USA). Absorbance was measured at 260 and 280 nm to determine a 260/280 ratio of 1.9 ± 0.1, which was used as quality cut-off, and a minimum extracted DNA concentration of 12 ng μL^{-1} was required to properly perform sequencing on the Illumina MiSeq platform by the Research and Testing Laboratory (Lubbock, Texas, USA). Bacterial 16S rRNA variable regions V4 were targeted using the primer pair 515F-806R for general bacteria.

2.4. Benchmarking of nitrogen valorization

A comparison, based on mass and energy balances, was made between four process configurations: (i) a conventional biological nitrogen removal system, i.e. nitrification/denitrification (N/DN) process; (ii) a process specifically designed for heterotrophic nitrogen recovery in the form of N_2O, i.e. the CANDO process; (iii) the PN-SBBR reactor presented in this study, devoted to autotrophic N_2O production, connected to a reactor for heterotrophic N_2O production (PN-N_2O/DN-N_2O) and (iv) the PN-SBBR reactor presented in this study, devoted to autotrophic N_2O production, connected to an Anammox reactor (PN-N_2O/A).

The mass and energy balances were calculated following a modified version of the procedure described in [21] under the following premises:

- The application of the four process configurations to the treatment of reject water from the dewatering of digested sludge with a nitrogen content of 1 kg $N\text{-}NH_4^+$ L^{-1} and without biodegradable organic matter.
- The N/DN process consists of a two-stage process: (i) a first nitrification reactor where the influent ammonium is completely oxidized to nitrate and (ii) a second denitrification reactor where the produced nitrate is completely reduced to dinitrogen gas with the addition of an external organic carbon source.
- The CANDO process consists of a two-stage process (i) a first nitritation reactor where the ammonium is completely oxidized to nitrite and (ii) a second denitritation reactor where the produced nitrite is partially reduced to nitrous oxide with the addition of an external organic carbon source.
- The PN-N_2O/DN-N_2O process consists of a two-stage process (i) a first PN-SBBR reactor, as the described in this study, where the ammonium is partially oxidized to nitrite with a significant production of nitrous oxide and (ii) a second denitritation reactor where the produced nitrite is partially reduced to nitrous oxide with the addition of an external organic carbon source.
- The PN-N_2O/A process consists of a two-stage process: (i) a first PN-SBBR, as the described in this study, where the ammonium is partially oxidized to nitrite with a significant production of nitrous oxide and (ii) a second Anammox reactor where the rest of ammonium and the produced nitrite are autotrophically transformed into dinitrogen gas.
- The efficiencies of N_2O production are based on experimental results: (i) 0.81 kg N-N_2O kg^{-1} $N\text{-}NH_4^+$ for CANDO and PN-N_2O/DN-N_2O processes [18] and (ii) 0.36 kg N-N_2O kg^{-1} $N\text{-}NH_4^+$ for PN-N_2O/A process (Table 1). It is assumed that the combined production of N_2O in the PN-N_2O/DN-N_2O process (autotrophic+heterotrophic) reaches the same total value as in the CANDO process.
- The organic matter required for heterotrophic denitrification in the N/DN, CANDO and PN-N_2O/DN-N_2O processes comes from a previous acidogenic fermentation stage of sewage sludge.
- The difference between the organic matter required for denitrification in the N/DN and CANDO processes is considered to be derived towards methane production in the CANDO process configuration.
- The difference between the organic matter required for denitrification in the N/DN and PN-N_2O/DN-N_2O processes is considered to be derived towards methane production in the PN- N_2O/DN-N_2O process configuration.
- The total organic matter required for denitrification in the N/DN process is considered to be derived towards methane production in the PN-N_2O/A configuration.
- The numerical factors used in the mass and energy balances calculation are: (1) ratio for ammonium oxidation to nitrate considering biomass production: 4.3 kg O_2 kg^{-1} N [22]; (2) ratio for ammonium oxidation to nitrite considering biomass production: 3.2 kg O_2 kg^{-1} N [22]; (3) ratio for nitrate reduction to dinitrogen gas considering biomass production: 4.1 kg COD kg^{-1} N [23]; (4) ratio for nitrite reduction to nitrous oxide considering biomass production: 2.5 kg COD kg^{-1} N [23]; (5) biomethane potential of sewage sludge: 0.12 m^3 CH_4 kg^{-1} COD [21]; (6) heat of methane combustion: 15.425 kWh kg^{-1} CH_4 [24]; (7) methane density: 0.717 kg CH_4 m^{-3} CH_4 (0 °C, 1 atm); (8) specific energy consumption for oxygen transfer: 1.0 kWh kg^{-1} O_2 [24]; (9) heat of nitrous oxide decomposition: 0.81 kWh kg N-N_2O [25].

A detailed description of the mass and energy balances, as well as the equations used for their calculation, can be found in the Supplementary data (Section 3).

Table 1
Summary of parameters and rates measured throughout the stable phases of each operational period. AOR: Ammonia oxidation rate, N2OR: N_2O production rate, $EF_{oxidized}$: Emission factor per nitrogen oxidized, EF_{load}: Emission factor per nitrogen loaded, DO: Dissolved oxygen concentration, NiAR: Nitrite accumulation rate and $FNA_{effluent}$: Free nitrous acid concentration in the effluent. Values are presented as mean ± standard deviation, with the coefficient of variation (%) shown in parentheses to indicate process stability.

Operational parameter	Units	Stable phases of the operational periods				
		I	II	III	II-bis	IV
pH	–	7.8 ± 0.1	7.3 ± 0.1	6.8 ± 0.1	7.3 ± 0.1	7.3 ± 0.1
AOR	g N L^{-1} d^{-1}	0.86 ± 0.03 (3.5)	0.89 ± 0.01 (1.1)	0.79 ± 0.01 (1.3)	0.90 ± 0.01 (1.1)	0.85 ± 0.02 (2.4)
N2OR	mg N L^{-1} d^{-1}	132 ± 13 (10)	230 ± 16 (7)	97 ± 8 (9)	217 ± 8 (4)	299 ± 7 (3)
$EF_{oxidized}$	% of mg N-N_2O mg^{-1} N-NH_4^+oxidized	16 ± 2 (10)	28 ± 2 (8)	12.1 ± 0.9 (8)	24.1 ± 0.8 (4)	36 ± 2 (6)
EF_{load}	% of mg N-N_2O mg^{-1} N-NH_4^+load	15 ± 2 (10)	27 ± 2 (8)	10.8 ± 0.9 (9)	23.1 ± 0.4 (2)	33.5 ± 0.8 (3)
NiAR	g N L^{-1} d^{-1}	0.79 ± 0.04 (5.1)	0.78 ± 0.02 (2.6)	0.90 ± 0.02 (2.2)	0.76 ± 0.01 (1.3)	0.71 ± 0.01 (1.4)
$FNA_{effluent}$	mg N L^{-1}	0.029 ± 0.001 (3.4)	0.088 ± 0.005 (5.7)	0.34 ± 0.06 (4.8)	0.078 ± 0.001 (1.3)	0.071 ± 0.003 (4.2)
DO	mg O_2 L^{-1}	2.2 ± 0.2 (9.1)	2.0 ± 0.2 (10)	2.1 ± 0.1 (4.8)	2.0 ± 0.2 (10)	1.4 ± 0.1 (7.1)

3. Results and discussion

3.1. Sustained N_2O production and comparison with previous studies

The PN-SBBR system demonstrated consistent and robust N_2O production without compromising PN performance under all tested conditions (Fig. 2, Table 1). Throughout the study (more than 300 days), the N2OR and $EF_{oxidized}$ spanned from 97 to 299 mg N-N_2O L^{-1} d^{-1} and 12 to 36%, respectively. While this range reflects the distinct pseudo-steady states induced by the applied pH setpoints, the system exhibited high stability within each individual period, as confirmed by the low intra-period coefficient of variation (Table 1). This pseudo-steady state performance contrasts with the N_2O emissions deterioration often reported in PN operations [26–28].

The highest N_2O production, feeding synthetic wastewater, occurred during period II under pH 7.3 (N2OR of 230 ± 16 mg N-N_2O L^{-1} d^{-1}, $EF_{oxidized}$ of 28 ± 2% and EF_{load} of 27 ± 2%). Remarkably, the use of real wastewater under the same pH caused an increase of the N_2O production (299 ± 7 mg N-N_2O L^{-1} d^{-1}, 36 ± 2% and 33.5 ± 0.7% as N2OR, $EF_{oxidized}$ and EF_{load}, respectively). The increase was attributed to the composition of the real wastewater matrix, specifically its organic matter content, as discussed later.

Only few studies have reported large N_2O productions ($EF_{oxidized}$ > 20%) in PN systems and these events were observed exclusively during short-term experiments conducted under transient disturbances (e.g. variations in nitrogen loading, DO concentration, temperature, or pH), which typically lead to temporarily increased N_2O productions [29,30]. Remarkably, stable values of N_2O production were obtained in the present study, falling within the upper range reported for short-term experiments in biofilm-based PN systems ($EF_{oxidized}$ 2–37%; in Table 2). Overall, the PN-SBBR consistently achieved high, stable and sustained N_2O production yields under PN conditions, highlighting its potential for nitrogen recovery-oriented applications.

Nitrous oxide production predominantly occurred during the aerated stages of the cycle ($N2OR_{aer}$ in Fig. 3), as reported in a similar activated sludge PN-SBR system [15]. Notably, the N2OR associated with the effluent ($N2OR_{liq}$) remained one order of magnitude lower than values

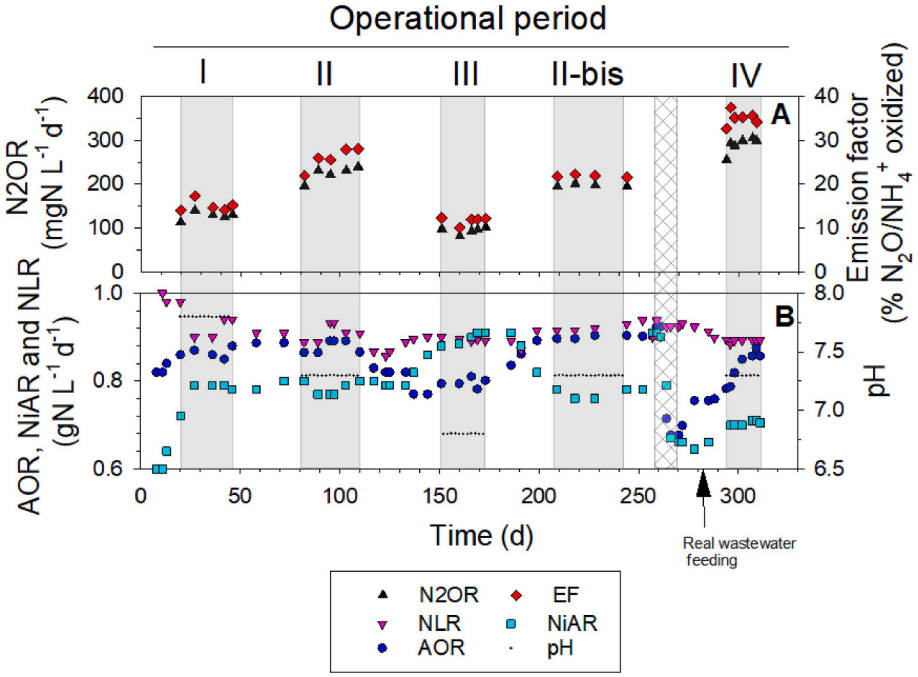


Fig. 2. Stable reactor operational phases (from operational periods I, II, III, II-bis and IV) are indicated by grey shading. The hatched area indicates a failure of the temperature control. Time course of: A) N_2O production rate (N2OR) and emission factor (EF). B) Nitrogen loading rate (NLR), ammonium oxidation rate (AOR) and nitrite accumulation rate (NiAR).

Table 2
Summary of the maximum emission factors (EF) and nitrous oxide production rate (N2OR) values reported in PN systems with both activated sludge and AGS (aerobic granular sludge), IFAS (integrated fixed-film activated sludge) and PN/A (partial nitritation plus Anammox) configuration studies. DO: dissolved oxygen concentration during the aerated stages; and T: temperature of the reactor; n.r.: not reported.

Operational system	Type of operation	Experimental conditions		N2OR (mg N L^{-1} d^{-1})	$EF_{oxidized}$ (%N_2O/$NH_{4\,oxidized}^{+}$)	EF_{load} (%N_2O/TN $_{load}$)	Ref.
		DO (mg O_2 L^{-1})	T (°C)				
IFAS	Short-term	0.5 ± 0.1	22 ± 1	n.r.	2.3	n.r.	[7]
AGS	Short-term	0.5–3	25 ± 1	205	37	n.r.	[32]
AGS	Short-term	1.1–4.5	30	n.r.	20	n.r.	[33]
Activated sludge	Short-term	0–3	22–23	115	10.4	n.r.	[34]
IFAS	Long-term	0.3 ± 0.1	22 ± 1	n.r.	1.1	n.r.	[7]
Activated sludge	Long-term	0.8 ± 0.2	20 ± 1	85	14	n.r.	[15]
Activated sludge	Long-term	0.3–0.8	20–26	44	8	7	[35]
AGS	Long-term	~0	30	94	14	13	[36]
PN-SBBR	Long-term	2.0–2.2	30 ± 1	299	36	34	This study

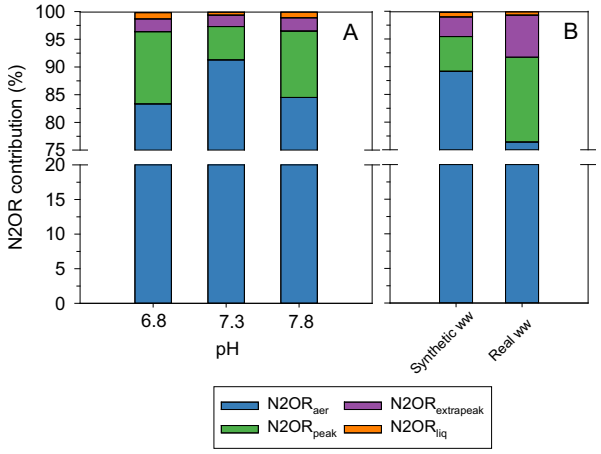


Fig. 3. N2OR fractional contribution of $N2OR_{aer}$—representing aerated stages excluding the N_2O peaks after aeration resumption—, $N2OR_{peak}$ and $N2OR_{extrapeak}$—representing N2OR contributions after the initial and interspersed aeration resumption, respectively—and $N2OR_{liq}$—representing the dissolved N_2O content in the effluent—to the total N2OR under stable reactor performance for: A) pH setpoint under synthetic wastewater feeding, and B) Different feeding conditions tested at pH 7.3.

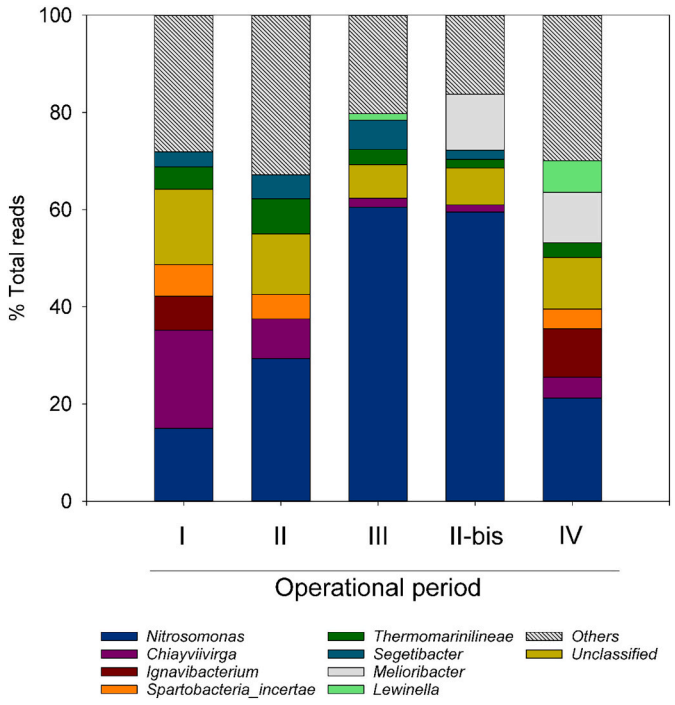


Fig. 4. Microbial relative abundance based on 16S rRNA sequencing at genus level. Unclassified and other fractions refer to unidentified 16S rRNA reads and below 5% of the total reads, respectively.

reported for an activated sludge PN-SBR system [15]. This difference should not be interpreted as enhanced N_2O consumption within the biofilm. Rather, activated sludge PN-SBRs are known to accumulate substantial amounts of N_2O in the bulk liquid during settling and other non-aerated periods [15], resulting in elevated dissolved N_2O concentrations prior to discharge. In the present PN-SBBR, dissolved N_2O represented less than approximately 1% of the total N_2O production under all tested conditions (Fig. 5.3), indicating limited N_2O accumulation in the bulk liquid before discharge. Consequently, N_2O losses via the effluent were substantially reduced, increasing the fraction of produced N_2O available in the reactor gas phase and thereby supporting future N_2O capture and recovery strategies.

Microbial community analysis based on 16S rRNA sequencing (Fig. 4) showed that *Nitrosomonas* genus remained the dominant AOB genus throughout all operational periods, despite variations in wastewater composition and reactor operating conditions. The persistence of the *Nitrosomonas* genus indicates a robust nitrifying consortium and supports its central role in sustained N_2O production. In the absence of external organic carbon during synthetic periods, N_2O production was likely dominated by AOB-mediated pathways, as widely reported for carbon-limited PN systems [31,32]. However, the active presence of heterotrophic bacteria (Fig. 4) suggests that they may play a minor role. Supported by decay products and soluble microbial products (SMP) as electron donor, these heterotrophs could contribute to the overall N_2O net balance, though further functional gene or isotopic analyses would be required to fully decouple these pathways [33].

The transition from synthetic to real sludge reject water in period IV introduced a more complex substrate matrix, triggering a noticeable decline in the relative abundance of AOB (Fig. 4). Although the potential presence of trace interfering compounds (e.g., heavy metals) cannot be entirely discarded [34], the discussion focused on the COD as carbon source that stimulated heterotrophic pathways, representing the main metabolic shift influencing N_2O dynamics between the synthetic and real wastewater periods.

Hence, the increase in the relative abundance of heterotrophic genera during period IV (such as *Ignavibacterium*, *Chiayviivirga* and *Lewinella* genera in Fig. 4) may explain both the 7% reduction in nitrite accumulation and the higher N_2O yields (increase of 38%) compared with those achieved using synthetic wastewater (Table 1). Considering these microbial population shifts, the enhanced N_2O production under real reject water conditions is likely linked to an interplay of heterotrophic activity. Given that heterotrophs can act as both N_2O producers and consumers [35], the higher N_2O production reported during period

IV suggests that under these specific operating conditions, N_2O production via heterotrophic denitrification pathways (stimulated by the incoming COD) outpaced biological N_2O consumption. Nevertheless, direct functional or isotopic evidence remains necessary to definitively confirm the precise metabolic contribution of these genera.

While taxonomic distribution provides a clear insight into the enrichment of key functional genera under different pH conditions, further molecular investigations—such as the quantification of functional genes and key enzymatic activities [36]—will be essential in future studies to investigate the active metabolic pathways at the transcriptomic level and avoid speculative attribution of pathway contributions.

Together, these results highlight the PN-SBBR as a novel operationally stable PN configuration and provide the basis for examining how bulk liquid pH modulates biofilm redox stratification and intermediates fate to control N_2O formation.

3.2. The pH effect on autotrophic N_2O production

The stable performance of PN-SBBR was evaluated under three different pH setpoints: 7.8 (period I), 7.3 (period II), and 6.8 (period III), exhibiting significant differences on the N_2O productions (one-way ANOVA, p value <0.001). A clear maximum in N_2O production was measured at pH 7.3 (Fig. 5A). Moreover, both the N2OR and EF values during period II-bis (also performed at pH 7.3, Fig. 2 and Table 1) were comparable to those measured during previous period II (Welch's t-test, $|t| < 2$, p value >0.05). This fact indicates that the effect of pH on autotrophic PN-driven N_2O production is consistent and reproducible. The low coefficients of variation (CV < 10%) observed within each operational period (Table 1), together with the absence of significant differences between period II and period II-bis according to Welch's t-test ($p > 0.05$), indicate that the pH effect on N_2O production was highly reproducible. These results suggest that any long-term changes in biofilm structure, biomass properties, or microbial composition did not substantially affect the observed process response under the tested conditions. Although prolonged operation under different pH conditions may have induced some degree of microbial adaptation before the pH was restored to 7.3 (see Fig. 4), the comparable N_2O responses observed in period II and period II-bis suggest that the pH effect was functionally reproducible. While complete preservation of microbial community composition cannot be guaranteed, deterministic environmental selection and functional redundancy are expected to promote convergence towards similar reactor performance under identical operating conditions [37–40].

Comparable AOR values were obtained at all pH levels, except at pH 6.3 (period III). Although FA may have contributed to some degree of AOB inhibition under the elevated ammonium concentrations applied, the observed decrease in ammonium oxidation rate with decreasing pH suggests that FA was not the dominant controlling factor. Since lower pH reduces FA concentrations while increasing FNA levels, the observed response is more consistent with FNA-related inhibition, although a contribution from FA cannot be completely excluded. However, substantial differences were observed in FNA and hydroxylamine concentrations in the bulk liquid between the different pH levels (one-way ANOVA, p value <0.001) (Fig. 5C and D). Taken together, these observations indicate that pH influenced the fate of N_2O-related intermediates, but did not substantially affect the AOR. The FNA concentration has been reported to inhibit AOB and its concentration in the effluent, i.e., at the end of the PN-SBBR cycle, increased markedly with decreasing pH (0.03, 0.09, and 0.3 mg N L^{-1} at pH 7.8, 7.3 and 6.8, respectively). Among these values, only the concentration reached at pH 6.8 can be considered inhibitory to AOB activity [41], which is consistent with the observed decrease in AOR (11% of reduction) during period III.

Under the tested system conditions, N_2O production was not governed by FNA alone, as reported in previous studies [42–44], but rather

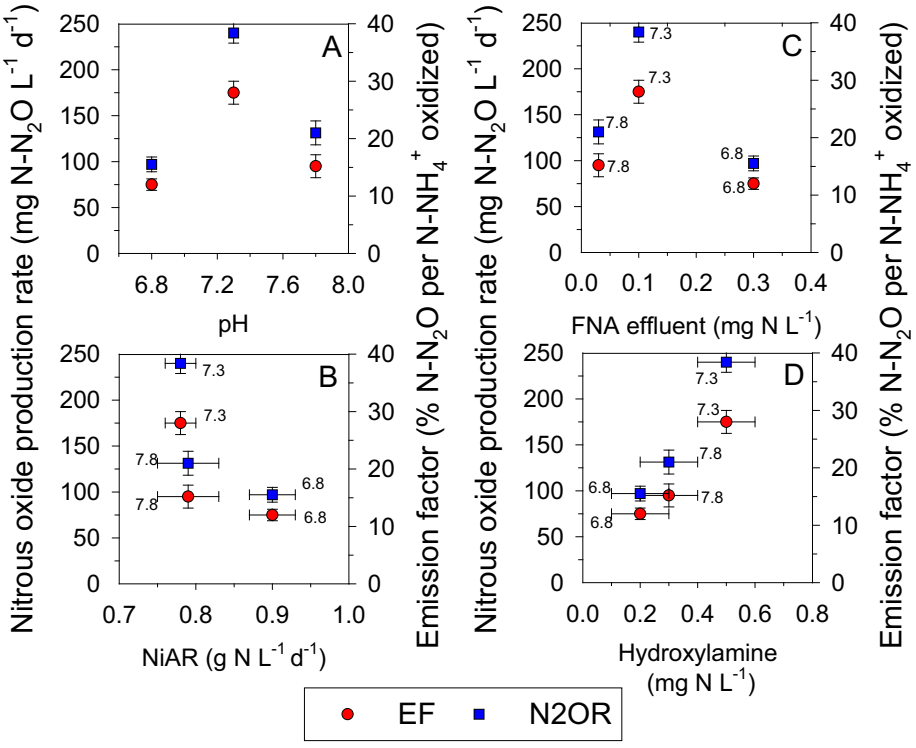


Fig. 5. Nitrous oxide production rate (N2OR) and emission factor (EF) reported during the stable phases of the first three operational periods tested with synthetic wastewater in relation to A) Bulk liquid pH in the reactor across reaction stage, B) Nitrite accumulation rate (NiAR) during the operational period, C) Average free nitrous acid (FNA) concentration in the effluent of the reactor and D) Hydroxylamine concentration detected in the bulk liquid during stable aerated stages of the cycle. The number next to each experimental point indicates the pH at which that value was obtained.

by its interaction with redox stratification and hydroxylamine availability. Modifications in oxygen penetration depth and redox stratification within the biofilm, are known to spatially decoupled hydroxylamine production and consumption [45,46]. This scenario was expected to shift electron portioning along biofilm depth from complete aerobic oxidation (nitrite redox state +3) towards truncated pathways, thereby promoting N_2O formation (redox state +1) [47,48]. Although the AOR and NiAR values at pH 7.8 (period I) were similar to those obtained at pH 7.3 (period II) (Table 1; $p > 0.05$), the hydroxylamine concentration in the bulk liquid was found to be significantly higher (Fig. 5D; $p < 0.01$) at pH 7.3. A deeper and smoother oxygen penetration at pH 7.3 could be expected (since at the biofilm surface the conditions are below the AOB optimal pH [17]) rising the extent of both active microaerobic and anoxic biofilm zones. The anoxic biofilm zones can be defined as areas with absence of oxygen but availability of hydroxylamine and FNA/nitrite as electron donor an acceptor, respectively. Under microaerobic conditions, AOB exhibited an increased N_2O yield per oxygen consumed (Olmo et al., unpublished results). Therefore, the expansion of microaerobic and anoxic biofilm zones could trigger N_2O formation pathways as supported by significant differences in N_2O production measured between these two periods ($p < 0.01$).

Hence, the pH 7.3 provides the most favorable redox conditions in which AOB ammonia oxidation activity is preserved while internal redox stratification and electron partitioning favor hydroxylamine-driven N_2O production in the PN-SBBR.

3.3. Perspectives on biological nitrogen valorization through autotrophic N_2O production

The sustained and stable N_2O production achieved by the PN-SBBR in the absence of external organic carbon, demonstrates the feasibility of autotrophic N_2O production as a nitrogen valorization strategy. This process could be applied for treating high-strength ammonium wastewater, such as reject water from dewatering of digested sludge. These results extend the role of PN beyond nitrogen removal, aligning with the emerging WRRF paradigm, in which nitrogen is recovered rather than eliminated as inert N_2.

Considering the conversion efficiencies achieved in the PN-SBBR, together with its energy requirements and ease of implementation, coupling the studied system with the Anammox process represents a practical option for further polishing the nitrogen content of the effluent. When the overall energy balance is compared per cubic meter of wastewater treated (Fig. 6), the PN-SBBR-Anammox configuration (PN-N_2O/A) has the potential to outperform conventional nitrification-denitrification (N/DN), CANDO and PN-N_2O/DN-N_2O processes. It should be highlighted that these energy balance calculations represent the maximum theoretical thermodynamic potential of each configuration under idealized, lossless conditions, rather than direct, net operational energy yields at full scale.

The PN-N_2O/A configuration combines autotrophic N_2O valorization with low-energy nitrogen polishing, thereby enhancing both energy recovery and process sustainability. From a practical standpoint, implementing the downstream Anammox stage for high-strength sludge reject water is highly feasible at full scale [49,50]. Despite the sensitivity of Anammox bacteria to low temperatures, the elevated temperature of incoming digested sludge reject water typically allows stable operation without external heating under insulated, near-adiabatic conditions. In contrast to the PN-N_2O/A configuration, which preserves organic matter for methane production, the CANDO process relies on organic carbon and therefore competes directly with anaerobic digestion for energy recovery, thus limiting its practical implementation [12,51]. Accordingly, the proposed two-stage system combining autotrophic PN-driven

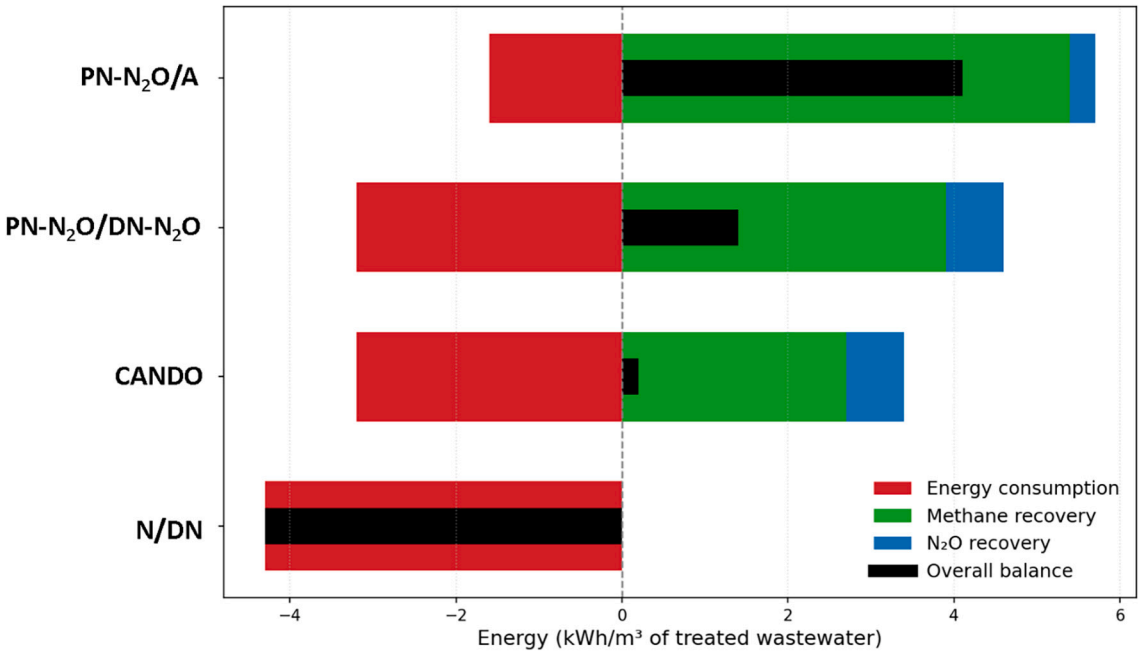


Fig. 6. Energy balance per process, including energy consumption, potential energy recovery from both methane and N_2O, respectively (described as methane and N_2O recoveries), and the overall balance. For each process configuration analyzed, the contributions from methane and N_2O recoveries are shown separately. Note that the aeration energy provided for partial nitritation natively drives in-situ N_2O stripping, and is therefore inherently included within the process energy consumption. The process configurations evaluated were: N/DN (a nitrification reactor where the influent ammonium is completely oxidized to nitrate followed by a denitrification reactor where the produced nitrate is completely reduced to N_2 with the addition of an external C-source); CANDO (a nitritation reactor where the ammonium is completely oxidized to nitrite followed by a denitritation reactor where the produced nitrite is partially reduced to N_2O with the addition of an external C-source); PN-N_2O/DN-N_2O (a PN-SBBR reactor, as the described in this study, where the ammonium is partially oxidized to nitrite with a significant production of N_2O followed by a denitritation reactor where the produced nitrite is partially reduced to N_2O with the addition of an external C-source); PN-N_2O/A (a PN-SBBR reactor, as the described in this study, where the ammonium is partially oxidized to nitrite with a significant production of N_2O followed by an Anammox reactor where the rest of ammonium and the produced nitrite are transformed into N_2). See numerical values in Supporting Information (Table S2).

N_2O production with Anammox avoids interfering with established anaerobic digestion schemes while introducing N_2O as an additional recoverable energy vector.

Despite the high N_2O yields observed, the PN-SBBR inherently retains a fraction of the nitrite produced during PN that is not directly converted to N_2O. Moreover, the CANDO process achieves higher overall yields (81% of N-N_2O produced per N-NO_2^- in the influent [52]) by coupling PN (without N_2O production) with heterotrophic nitrous oxide denitritation, converting nitrite to N_2O using organic matter. This comparison highlights a clear opportunity: decoupling autotrophic N_2O production from heterotrophic nitrite reduction. By introducing a dedicated denitritation stage downstream of the PN-SBBR, the residual nitrite could be further transformed into N_2O, creating a two-stage system in which both reactors act as complementary N_2O sources (PN-N_2O/DN-N_2O in Fig. 6). This configuration (PN-N_2O/DN-N_2O) exhibited higher N_2O recovery than the PN-N_2O/A configuration (57% increase); however, the organic matter requirement penalized the overall energy balance (66% reduction).

Beyond energy potential, the PN-SBBR offers a key operational advantage: aerated conditions inherently promote in situ N_2O stripping and air-enrichment, avoiding the need for dedicated, secondary gas stripping units and thereby reducing overall separation costs [53,54]. Consequently, the energy required for gas stripping was directly coupled with the baseline aeration demands of the partial nitritation stage itself. The low N_2O discharge via the effluent observed in this study (Fig. 3) further supports the suitability of this biofilm-based PN system for gas-phase N_2O recovery and valorization.

Overall, integrating a PN-SBBR as a first, predominantly autotrophic N_2O-producing and gas-stripping unit, followed by a secondary either Anammox or heterotrophic denitritation reactor to convert residual nitrite, represents a high-performance and WRRF-compatible nitrogen valorization strategy. These hybrid configurations maximize N_2O recovery, preserve organic matter for methane production, and exploit the intrinsic advantages of biofilm systems to enable efficient and scalable N_2O valorization. Consequently, mitigating environmental risks represents a fundamental prerequisite for full-scale implementation; key challenges for implementation include safe N_2O handling, gas upgrading, and process control to avoid uncontrolled emissions, which warrant further investigation.

4. Conclusions

The PN-SBBR achieved sustained and reproducible N_2O production without compromising partial nitritation, reaching ammonium to N_2O conversions of up to 36% and production rates of 299 mg N-N_2O L^{-1} d^{-1} under stable operation. Unlike transient emissions peaks previously reported in the literature, high N_2O yields were maintained over the long term, demonstrating the robustness of the process.

Bulk liquid pH emerged as the key operational control variable, with pH 7.3 identified as the most favorable among the tested range, under which ammonium oxidation remained preserved while biofilm redox stratification and hydroxylamine availability maximized N_2O formation. Operation with real reject water further enhanced N_2O yields (+38%), likely associated with the increased contribution of heterotrophic pathways to N_2O production.

Positioning the PN-SBBR as a first-stage autotrophic N_2O-producing and gas-stripping unit, coupled with downstream Anammox or heterotrophic denitritation, opens a new pathway for nitrogen valorization. This configuration redefines PN from nitrogen-removal step to a platform for controlled energy-vector generation, thereby aligning PN within the WRRF paradigm.

CRediT authorship contribution statement

Lluc Olmo: Writing – original draft, Methodology, Investigation, Formal analysis, Data curation. **Julio Pérez:** Writing – review & editing, Supervision, Investigation, Funding acquisition. **Julián Carrera:** Writing – review & editing, Supervision, Project administration, Investigation, Funding acquisition.

Declaration of competing interest

The authors declare that they have no known competing financial interests or personal relationships that could have appeared to influence the work reported in this paper.

Acknowledgements

This work was supported by the grants ORIGEN PID2021-126102OBI00 and BioN2O PID2024-159120OB-I00 funded by MCIN/AEI/10.13039/501100011033 and by ERDF: A way of making Europe from the European Union. Lluc Olmo also acknowledges a predoctoral grant from Universitat Autonòma de Barcelona (PIF 2021–2022). The authors are members of the GENOCOV research group, Consolidated Research Group of the Generalitat de Catalunya. All the authors are members of the Iberoamerican Biofuturo CYTED network (424RT0157).

Appendix A. Supplementary data

Supplementary data to this article can be found online at https://doi.org/10.1016/j.cej.2026.180743.

Data availability

Data will be made available on request.

References

[1] N.T. Bahgat, P. Wilfert, L. Korving, M. Van Loosdrecht, Integrated resource recovery from aerobic granular sludge plants, Water Res. 234 (2023) 119819, https://doi.org/10.1016/j.watres.2023.119819.
[2] R. Pott, M. Johnstone-Robertson, B. Verster, S. Rumjeet, L. Nkadimeng, T. Raper, S. Rademeyer, S.T.L. Harrison, Wastewater Biorefineries: Integrating Water Treatment and Value Recovery, in: Green Energy Technol., Springer Verlag, 2018, pp. 289–302, https://doi.org/10.1007/978-3-319-63612-2_18.
[3] N. Horstmeyer, M. Weißbach, K. Koch, J.E. Drewes, A novel concept to integrate energy recovery into potable water reuse treatment schemes water reuse treatment schemes, J. Water Reuse Desalination (2017), https://doi.org/10.2166/wrd.2017.051.
[4] P.L. McCarty, J. Bae, J. Kim, Domestic wastewater treatment as a net energy producer-can this be achieved? Environ. Sci. Technol. 45 (2011) 7100–7106, https://doi.org/10.1021/es2014264.
[5] M. Maurer, P. Schwegler, T.A. Larsen, Nutrients in urine: energetic aspects of removal and recovery, Water Sci. Technol. 48 (2002) 37–46.
[6] J.M. Blum, M.M. Jensen, B.F. Smets, Nitrous oxide production in intermittently aerated partial Nitritation-Anammox reactor: oxic N2O production dominates and relates with ammonia removal rate, Chem. Eng. J. 335 (2018) 458–466, https://doi.org/10.1016/j.cej.2017.10.146.
[7] Y. He, X. Yang, Y. Jin, Y. Liu, Y. Wang, T. Zhu, B. Ni, Y. Liu, Biofilm increases N2O production in a sidestream partial nitritation system under low dissolved oxygen conditions, Water Res. 290 (2026) 125077, https://doi.org/10.1016/j.watres.2025.125077.
[8] K.O. Denisov, A.A. Ilyin, R.N. Rumyantsev, A.P. Ilyin, A.V. Volkova, Nitrous oxide: production, application, and protection of the environment, J. Gen. Chem. 89 (2019) 1338–1346, https://doi.org/10.1134/S107036321906032X.
[9] M. Weißbach, P. Thiel, J.E. Drewes, K. Koch, Nitrogen removal and intentional nitrous oxide production from reject water in a coupled nitritation/nitrous denitritation system under real feed-stream conditions, Bioresour. Technol. 255 (2018) 58–66, https://doi.org/10.1016/j.biortech.2018.01.080.
[10] Y.D. Scherson, S.G. Woo, C.S. Criddle, Production of nitrous oxide from anaerobic digester centrate and its use as a co-oxidant of biogas to enhance energy recovery, Environ. Sci. Technol. 48 (2014) 5612–5619, https://doi.org/10.1021/es501009j.
[11] Y.D. Scherson, G.F. Wells, S. Woo, J. Lee, J. Park, J. Cantwell, C.S. Criddle, Nitrogen removal with energy recovery through N2O decomposition, Energy Environ. Sci. (2013) 241–248, https://doi.org/10.1039/c2ee22487a.
[12] M. Zhang, J. Gu, Y. Liu, Engineering feasibility, economic viability and environmental sustainability of energy recovery from nitrous oxide in biological wastewater treatment plant, Bioresour. Technol. 282 (2019) 514–519, https://doi.org/10.1016/j.biortech.2019.03.040.
[13] W. Kuai, L., Verstraete, Ammonium removal by the oxygen-limited autotrophic nitrification-denitrification system, Appl. Environ. Microbiol. 64 (1998) 4500–4506, https://doi.org/10.1128/AEM.64.11.4500-4506.1998.

[14] A. Soler-Jofra, R. Wang, R. Kleerebezem, M.C.M. Van Loosdrecht, Stratification of nitrifier guilds in granular sludge in relation to nitritation, Water Res. 148 (2019) 479–491, https://doi.org/10.1016/j.watres.2018.10.064.
[15] L. Olmo, J. Carrera, J. Pérez, Nitrous oxide production and hydroxylamine accumulation in a partial nitritation sequencing batch reactor: comparison of different operational strategies, ACS EST Water 6 (2026) 164–172, https://doi.org/10.1021/acsestwater.5c00856.
[16] H. Horn, C.H. Dietmar, Growth and decay in an auto−/heterotrophic biofilm, Water Res. 31 (1997) 2243–2252, https://doi.org/10.1016/S0043-1354(97)00081-X.
[17] S. Park, W. Bae, B.E. Rittmann, Multi-species nitrifying biofilm model (MSNBM) including free ammonia and free nitrous acid inhibition and oxygen limitation, Biotechnol. Bioeng. 105 (2010), https://doi.org/10.1002/bit.22631.
[18] M. Weber, B., Juanico, Variability of effluent quality in a multi-step complex for wastewater treatment and storage, Eng. Water Resour. 24 (1990) 765–771, https://doi.org/10.1016/0043-1354(90)90034-4.
[19] J. Foley, D. De Haas, Z. Yuan, P. Lant, Nitrous oxide generation in full-scale biological nutrient removal wastewater treatment plants, Water Res. 44 (2010) 831–844, https://doi.org/10.1016/j.watres.2009.10.033.
[20] R. Marques, A. Rodriguez-Caballero, A. Oehmen, M. Pijuan, Assessment of online monitoring strategies for measuring N2O emissions from full-scale wastewater treatment systems, Water Res. 99 (2016) 171–179, https://doi.org/10.1016/j.watres.2016.04.052.
[21] J. Carrera, O. Carbó, S. Doñate, M.E. Suárez-Ojeda, J. Pérez, Increasing the energy production in an urban wastewater treatment plant using a high-rate activated sludge: pilot plant demonstration and energy balance, J. Clean. Prod. 354 (2022) 131734, https://doi.org/10.1016/j.jclepro.2022.131734.
[22] C.T. Wezernak, G.J. J, Oxygen-nitrogen relationships in autotrophic nitrification, Appl. Microbiol. 15 (1967) 1211–1215.
[23] C. Ramos, M.E. Suárez-ojeda, J. Carrera, Denitritation in an anoxic granular reactor using phenol as sole organic carbon source, Chem. Eng. J. 288 (2016) 289–297, https://doi.org/10.1016/j.cej.2015.11.099.
[24] G. Tchobanoglous, F.L. Burton, H.D. Stensel, Metcalf & Eddy, Inc., Wastewater Engineering: Treatment and Reuse, McGraw-Hil, Boston, 2003.
[25] Y. Yamamoto, T. Tachibana, Decomposition promotion of nitrous oxide for its use as an energy carrier, Fuel 364 (2024) 131055, https://doi.org/10.1016/j.fuel.2024.131055.
[26] V. Vasilaki, V. Conca, N. Frison, A.L. Eusebi, F. Fatone, E. Katsou, A knowledge discovery framework to predict the N2O emissions in the wastewater sector, Water Res. 178 (2020) 115799, https://doi.org/10.1016/j.watres.2020.115799.
[27] W. Gruber, R. Niederdorfer, J. Ringwald, E. Morgenroth, H. Bürgmann, A. Joss, Linking seasonal N2O emissions and nitrification failures to microbial dynamics in a SBR wastewater treatment plant, Water Res. X 11 (2021) 100098, https://doi.org/10.1016/j.wroa.2021.100098.
[28] N. Uri-Carreño, P.H. Nielsen, K.V. Gernaey, C. Domingo-Félez, X. Flores-Alsina, Nitrous oxide emissions from two full-scale membrane-aerated biofilm reactors, Sci. Total Environ. 908 (2024), https://doi.org/10.1016/j.scitotenv.2023.168030.
[29] J.M. Ribeiro, V. Conca, J.M.M. Santos, D.F.C. Dias, N. Sayi-Ucar, N. Frison, A. Oehmen, Expanding ASM models towards integrated processes for short-cut nitrogen removal and bioplastic recovery, Sci. Total Environ. 821 (2022) 153492, https://doi.org/10.1016/j.scitotenv.2022.153492.
[30] M. Zheng, J. Lloyd, P. Wardrop, H. Duan, T. Liu, L. Ye, B.J. Ni, Path to zero emission of nitrous oxide in sewage treatment: is nitrification controllable or avoidable? Curr. Opin. Biotechnol. 91 (2025) 103230 https://doi.org/10.1016/j.copbio.2024.103230.
[31] A. Rosa-Masegosa, A. Rodriguez-Sanchez, S. Gorrasi, M. Fenice, A. Gonzalez-Martinez, J. Gonzalez-Lopez, B. Muñoz-Palazon, Microbial ecology of granular biofilm technologies for wastewater treatment: a review, Microorganisms (2024) 1–22, https://doi.org/10.3390/microorganisms12030433.
[32] B. Read-Daily, S. Ben Maamar, F. Sabba, S. Green, R. Nerenberg, Effect of nitrous oxide (N2O) on the structure and function of nitrogen-oxide reducing microbial communities, Chemosphere 307 (2022) 135819, https://doi.org/10.1016/j.chemosphere.2022.135819.
[33] E. Harris, A. Joss, L. Emmenegger, M. Kipf, B. Wolf, J. Mohn, P. Wunderlin, Isotopic evidence for nitrous oxide production pathways in a partial nitritation-anammox reactor, Water Res. 83 (2015) 258–270, https://doi.org/10.1016/j.watres.2015.06.040.
[34] Q. Su, C. Domingo-Félez, M.M. Jensen, B.F. Smets, Abiotic nitrous oxide (N2O) production is strongly pH dependent, but contributes little to overall N2O emissions in biological nitrogen removal systems, Environ. Sci. Technol. 53 (2019) 3508–3516, https://doi.org/10.1021/acs.est.8b06193.
[35] H. Gao, Y. Mao, X. Zhao, W.T. Liu, T. Zhang, G. Wells, Genome-centric metagenomics resolves microbial diversity and prevalent truncated denitrification pathways in a denitrifying PAO-enriched bioprocess, Water Res. 155 (2019) 275–287, https://doi.org/10.1016/j.watres.2019.02.020.
[36] B. Kartal, H.J.C.T. Wessels, E. van der Biezen, K.J. Francoijs, M.S.M. Jetten, M. G. Klotz, L.Y. Stein, Effects of nitrogen dioxide and anoxia on global gene and protein expression in long-term continuous cultures of Nitrosomonas eutropha C91, Appl. Environ. Microbiol. 78 (2012) 4788–4794, https://doi.org/10.1128/AEM.00668-12.
[37] D.C. Vuono, J. Benecke, J. Henkel, W.C. Navidi, T.Y. Cath, J. Munakata-marr, J. R. Spear, Disturbance and temporal partitioning of the activated sludge metacommunity, ISME J. 9 (2015) 425–435, https://doi.org/10.1038/ismej.2014.139.
[38] M. De Celis, A. Santos, J. Duque, D. Marquina, H. Salvadó, I. Belda, Niche differentiation drives microbial community assembly and succession in full-scale activated sludge bioreactors, Nat. Biofilms Microbiomes 23 (2022) 1–6, https://doi.org/10.1038/s41522-022-00291-2.
[39] I. Hayashi, H. Fujita, H. Toju, Deterministic and stochastic processes generating alternative states of microbiomes, ISME Commun. 4 (2024).
[40] H. Fujita, M. Ushio, K. Suzuki, M.S. Abe, M. Yamamichi, K. Iwayama, Alternative stable states, nonlinear behavior, and predictability of microbiome dynamics, Microbiome 11 (2023) 1–16, https://doi.org/10.1186/s40168-023-01474-5.
[41] J.A. Torà, J. Lafuente, J.A. Baeza, J. Carrera, Combined effect of inorganic carbon limitation and inhibition by free ammonia and free nitrous acid on ammonia oxidizing bacteria, Bioresour. Technol. 101 (2010) 6051–6058, https://doi.org/10.1016/j.biortech.2010.03.005.
[42] O. Kinnunen, A. Kruglova, M. Mark, A. Kuokkanen, B.F. Smets, A. Mikola, Shift in activated sludge microbiomes associated with nitrite accumulation and high nitrous oxide emissions, Environ. Res. 277 (2025) 121591, https://doi.org/10.1016/j.envres.2025.121591.
[43] C. Picioreanu, M.C.M. Van Loosdrecht, Modelling the effect of oxygen concentration on nitrite accumulation in a biofilm airlift suspension reactor, Water Sci. Technol. 36 (1997) 147–156, https://doi.org/10.1016/S0273-1223(97)00347-8.
[44] H. Duan, Q. Wang, D.V. Erler, L. Ye, Z. Yuan, Effects of free nitrous acid treatment conditions on the nitrite pathway performance in mainstream wastewater treatment, Sci. Total Environ. 644 (2018) 360–370, https://doi.org/10.1016/j.scitotenv.2018.06.346.
[45] W.F. Harper, A. Terada, F. Poly, X. Le Roux, K. Kristensen, M. Mazher, B.F. Smets, The effect of hydroxylamine on the activity and aggregate structure of autotrophic nitrifying bioreactor cultures, Biotechnol. Bioeng. 102 (2009) 714–724, https://doi.org/10.1002/bit.22121.
[46] F. Sabba, C. Picioreanu, J. Pérez, R. Nerenberg, Hydroxylamine diffusion can enhance N2O emissions in nitrifying biofilms: a modeling study, Environ. Sci. Technol. 49 (2015) 1486–1494, https://doi.org/10.1021/es5046919.
[47] M.N. Young, J. Boltz, B.E. Rittmann, A. Al-Omari, J.A. Jimenez, I. Takacs, A. K. Marcus, Thermodynamic analysis of intermediary metabolic steps and nitrous oxide production by ammonium-oxidizing Bacteria, Environ. Sci. Technol. 56 (2022) 12532–12541, https://doi.org/10.1021/acs.est.1c08498.
[48] M. Spérandio, L. Lang, F. Sabba, R. Nerenberg, P. Vanrolleghem, C. Domingo-Félez, B.F. Smets, H. Duan, B.-J. Ni, Z. Yuan, Modelling N2O production and emissions, in: Quantif. Model. Fugitive Greenh. Gas Emiss. From Urban Water Syst., IWA Publishing, 2022, pp. 167–196, https://doi.org/10.2166/9781789060461_0167.
[49] S. Lackner, E.M. Gilbert, S.E. Vlaeminck, A. Joss, H. Horn, M.C.M. Van Loosdrecht, Full-scale partial nitritation/anammox experiences-An application survey, Water Res. 55 (2014) 292–303, https://doi.org/10.1016/j.watres.2014.02.032.
[50] B. Kartal, J.K. Kuenen, M.C.M. van Loosdrecht, Sewage treatment with anammox, Science 328 (2010) 702–703, https://doi.org/10.1126/science.1185941 (80-.).
[51] H. Zhou, Z. Wang, S. Pan, P. Rezazadeh, W. Zhang, M.C. Mc, Benchmarking sidestream shortcut nitrogen removal processes against nitrous oxide recovery from a life cycle perspective, J. Clean. Prod. 384 (2023) 135530, https://doi.org/10.1016/j.jclepro.2022.135530.
[52] Z. Wang, S.G. Woo, Y. Yao, H.H. Cheng, Y.J. Wu, C.S. Criddle, Nitrogen removal as nitrous oxide for energy recovery: increased process stability and high nitrous yields at short hydraulic residence times, Water Res. 173 (2020), https://doi.org/10.1016/j.watres.2020.115575.
[53] H. Duan, Y. Zhao, K. Koch, G.F. Wells, M. Weißbach, Z. Yuan, Recovery of nitrous oxide from wastewater treatment: current status and perspectives, ACS EST Water 1 (2021) 240–250, https://doi.org/10.1021/acsestwater.0c00140.
[54] M. Weißbach, F. Gossler, J.E. Drewes, K. Koch, Separation and Puri fi cation technology separation of nitrous oxide from aqueous solutions applying a micro porous hollow fi ber membrane contactor for energy recovery, Sep. Purif. Technol. 195 (2018) 271–280, https://doi.org/10.1016/j.seppur.2017.12.016.